Effect of layered silicates on fibril formation and properties of PCL/PLA microfibrillar composites

Ivan Kelnar, Ivan Fortelný, Ludmila Kaprálková, Jaroslav Kratochvíl, Borislav Angelov, Martina Nevoralová

Institute of Macromolecular Chemistry, Academy of Sciences of the Czech Republic, Praha 162 06, Czech Republic
Correspondence to: I. Kelnar (E-mail: kelnar@imc.cas.cz)

ABSTRACT: The study deals with improvement of poly(ε-caprolactone) (PCL) parameters by *in situ* forming of poly(lactic acid) (PLA) fibrils. This structure is achieved by preparation of the melt-drawn microfibrillar composite (MFC) from the PCL/PLA 80/20 blend containing the organophilized montmorillonite (oMMT) added using various mixing protocols. Improved mechanical behavior corresponds to the micron-sized fibrils formation and reinforcement of both polymer components by oMMT, and to increased crystalline phase content in the fibrillar PLA phase. Effective melt drawing is only possible after the rheological parameters of the polymer components have been modified by oMMT where the clay addition method and content are of primary importance. From the results obtained, it follows that the role of oMMT in MFC is quite complex, numerous clay-induced effects may be contradictory and must be harmonized to achieve PCL-based biodegradable MFCs with improved parameters. © 2015 Wiley Periodicals, Inc. J. Appl. Polym. Sci. **2016**, *133*, 43061.

INTRODUCTION

Poly(ε-caprolactone) is a biodegradable material with many advantageous features for biomedical, packaging, and other applications. However, its range of applications is limited by low yield stress, stiffness, and highly ductile deformation under ambient conditions.[1] The reason is combination of low glass transition temperature and less stable crystalline structure. Mechanical behavior can be optimized by blending, optimally using a suitable biodegradable polymer to preserve biodegradability. Examples are blends with relatively rigid poly(lactic acid) (PLA).[2–7] In spite of similar structure, fair compatibility only occurs in combination of PCL with PDLLA containing 12 mol % of D-lactide isomer.[4] Blends of PCL/commercial PLA containing ∼4% of this isomer have relatively low compatibility; therefore, some compatibilizing techniques have to be applied.[6,7] Generally, the potential of improving mechanical properties of PCL using blending is relatively low.

Another method of enhancing PCL mechanical behavior is preparation of composites using, e.g., PLA-based fibers,[8] predominantly prepared via electrospinning.[9,10] Combinations of PCL with various short fibers of natural origin, such as chitin fibers,[11] abaca,[12] and silk fibroin,[13] are reported as well. Especially application of electrospun fibers is accompanied by processing limitations practically excluding use of traditional thermoplastic processing techniques, such as injection molding. As a result, the reinforcing potential of fibers is usually not fully exploited due to difficult dispergation of polymeric fibers and low adhesion between fibers and matrix.[14] Therefore, fiber and/or matrix modifications are necessary.[14] An effective alternative is application of nanofillers (NFs),[15–17] preferably layered silicates, with better dispersion and thus improved mechanical behavior achieved in the case of *in situ* polymerization techniques.[18] Recently, Lee and Chang[19] reported on significant improvement of mechanical properties of PCL using unmodified halloysite. In spite of fourfold increase in stiffness, elongation, and stress at break, this material still possesses significant PCL limitations for many application areas, i.e., relatively low yield strength combined with undesirable drawability. Similar high ductility was observed by Neppali in oMMT-based nanocomposite (NC).[20]

A promising method to achieve better balanced mechanical performance is application of a polymer blend and a NF.[21–23] An example is the PCL/PLA system containing microtalc[24] and NFs, such as oMMT;[25] however, most of the published articles deal with PLA matrix modified with a low amount of PCL.[26,27] An efficient method to prepare short-fiber composites is the concept of microfibrillar composites (MFC),[28–31] i.e., *in situ* preparation of short-fibers by melt or cold drawing of polymer

blends. The *in situ* fiber formation leads to fair fiber dispergation and adhesion which may be promoted by transcrystallinity.[31] Of importance is the fact that the fibril-forming rigid polymer, preferably semicrystalline, has markedly higher melting point than the processing temperature of the matrix, such as HDPE/PA6. In this case, the drawn blend may be subsequently processed using conventional techniques.

Limitations of MFC, like low mechanical parameters and dimensional stability at elevated temperatures, can be eliminated by simultaneous application of NF. In the case of carbon nanotubes, the published articles report on limitation of fibril formation in PE/PET systems[32] and unexpected practically no improvement of mechanical properties in PP/PA66 system,[33] in spite of fibril formation. Our study on HDPE/PA6/oMMT composite[34] has shown both improved mechanical behavior and also parameters lower than the analogous clay-free MFC (close to HDPE matrix). This confirms the fact that the effect of NF on structure and properties of MFC is quite complex, with expected occurrence of contradictory effects. Moreover, oMMT can influence parameters (dimensions) of fibrils as well. Surprisingly, the best behavior was found in the case of fibrils with the highest diameter and rather lower aspect ratio (AR); but the dimensions were within a favorable range known for analogous short fiber composites.[35] Moreover, the importance of AR in the composite with relatively low difference of component parameters is less pronounced. We tentatively ascribe the mentioned variations in mechanical behavior of MFC to crucial importance of clay-affected parameters of the interface. Significant reduction in stiffness due to a thin low-modulus interlayer was found for carbon fiber composites[36]; according to our preliminary results of finite element analysis, this effect can also occur in polymer fiber-reinforced MFC.

Due to a relatively large number of biodegradable polyesters, application of the MFC concept to the PCL matrix with low processing temperature ($\sim$130°C) can be an advanced efficient alternative to the mentioned natural fiber-based composites.[11–13] In this area, preparation of PLA/poly(glycolic acid) melt-drawn MFC for medical applications,[37,38] not processed via melting-based techniques like injection molding, are reported. Preparation of PLA microfibers via stretching of a suitable blend with copolyester[39] and poly(ethylene-vinylalcohol) copolymer[40] followed by matrix extraction has also been reported. Another similar systems are PCL-blend fibers and analogous blend fibers with halloysite prepared by electrospinning.[41,42] Based on the above overview and to the best of our knowledge, the PCL-matrix MFC has not yet been reported in the literature. Therefore, the present study addresses MFC based on the PCL/PLA 80/20 combination and the analogous oMMT-modified MFC in order to prepare a biodegradable system with improved mechanical properties.

EXPERIMENTAL

Materials

Poly(lactic acid) (PLA) Ingeo 2002D (NatureWorks) with the D-isomer content of 4.3%, M_w 2.53 × 10^5 g mol^{-1}, melt flow rate 6 g/10 min (190°C/2.16 kg), and density 1.24 g cm^{-3}. Poly(ε-caprolactone) (PCL) CAPA 6800 (Perstorp) M_n 8 × 10^4 g mol^{-1}, density 1.145 g cm^{-3}. Clays based on natural montmo-

rillonite: Cloisite 15A modified with dialkyldimethylammonium chloride 95-meq/100-g (C15); Cloisite 30B modified with alkyl-bis(2-hydroxyethyl)dimethylammonium chloride 90-meq/100-g, with alkyl derived from tallow (C30, Southern Clay Products).

MFC Preparation

Prior to mixing, PCL, PLA, and clay were dried at 45, 85, and 70°C, respectively, in a vacuum oven for 12 h. The mixing was carried out in a counter-rotating segmented twin-screw extruder (L/D 40) Brabender TSE 20 at 400 rpm, and temperatures of the respective zones (from feeding to die) of 170, 170, 170, 170, 175, and 180°C. The extruded bristle with the PCL/PLA 80/20 w/w composition was melt-drawn using an adjustable take-up device. The draw ratio (DR) is the ratio between the velocity of the take-up rolls and the initial velocity of the extruded bristle, DR 5 and 7 were mostly used. In addition to the one-step addition of all components (with 2 phr clay addition), preblends of PCL with 3% C15 and PLA with 1% C15 were also applied. The PCL preblend was mixed using temperatures 135°C in all zones, the PLA preblend was mixed using temperature profile 185, 190, 190, 190, 190, and 190°C. Dog-bone specimens (gauge length 40 mm) were prepared in a laboratory microinjection molding machine (DSM). The barrel and the mold temperatures were 137 and 30°C, respectively.

Testing

Tensile tests were carried out using an Instron 5800 apparatus at 22°C and crosshead speed of 20 mm/min. At least eight specimens were tested for each sample. Young's modulus (E), maximum stress (σ_m), and elongation at break (ε_b) were evaluated; the corresponding variation coefficients did not exceed 10, 2, and 20%, respectively.

Tensile impact strength, a_b was measured on one-side notched specimens using a Zwick hammer with energy of 4 J (variation coefficient 10–15%). The reported values are averages of twelve individual measurements. The differential scanning calorimetry (DSC) analysis was carried out using a Perkin-Elmer 8500 DSC apparatus. Samples of 5 – 10 mg were heated from 50 to 250°C at the heating rate of 10°C/min. The melting temperature T_m was identified as the melting endotherm maximum. The crystallinity was calculated using the values 139.5 and 93.1 J/g for the heat of melting of 100%-crystalline PCL and PLA, respectively.

Characterization of Structure

The structure of drawn and undrawn samples was examined using scanning electron microscopy (SEM) with a Vega (Tescan) microscope. The injection molded specimens of undrawn blends were broken under liquid nitrogen. Because of impossibility of PLA fibrils extraction due to chemical similarity of both polyesters, the drawn bristle samples were broken under liquid nitrogen in parallel direction with respect to their long axis. The PLA phase was etched using 20% NaOH at room temperature for 30min; this visualization is based on faster hydrolysis of PLA in comparison with PCL. For the transmission electron microscope (Tecnai) observations, ultrathin (60 nm) sections were prepared under liquid nitrogen using an Ultracut UCT (Leica) ultramicrotome. To improve contrast between polymer components, uranyl acetate-staining was also applied, unfortunately without effect.

Wide-angle X-ray scattering (WAXS) experiments were performed using a pinhole camera (Molecular Metrology System, Rigaku, Japan) attached to a microfocused X-ray beam generator (Osmic MicroMax 002) operating at 45 kV and 0.66 mA (30 W). The camera was equipped with removable and interchangeable imaging plate 23 × 25 cm (Fujifilm). Experimental setup covered the momentum transfer (q) range of 0.25–3.5 Å^{-1}. $q = (4\pi/\lambda)\sin\theta$, where $\lambda = 1.54$ Å is the wavelength and 2θ is the scattering angle. Calibrations of the centre and sample-to-detector distance were made using Si powder. Samples were measured in the transmission mode. In the XRD patterns, the interlayer spacing of clay was determined from the 2θ position of the peak corresponding to the {001} basal reflection of montmorillonite (referred to as d_{001} peak).

Rheological Characterization

Rheological characterization was conducted using an ARES apparatus (Rheometric Scientific, Piscataway, NJ) with the parallel-plate geometry at 137 and 170°C using an oscillatory shear deformation at frequency of 6.2 rad/s. The amplitude of oscillation was 3%, i. e. within the range of linear viscoelasticity of all studied materials.

RESULTS AND DISCUSSION

Effect of Clay on PLA Fibril Formation

Mixing and subsequent extrusion of the PCL/PLA 80/20 blend through a round die lead to the bristle with relatively low melt strength; moreover the extrusion was unstable—variable bristle diameter. As a result, melt drawing of the clay-free blend was impossible. This most probably corresponds to unfavorable combination of rheological parameters.[29] Similar extrusion behavior was found for other blends of PCL with three PLA types of different characteristics (not shown). The addition of C15 or C30 using various mixing protocols leads to an improved extrusion process and successful melt drawing. This also corresponds to increased viscosity of the clay-containing blend in comparison with the clay-free blend (see below). The formation of the PLA fibrils is obvious from the SEM image [Figure 1(a,b)]. Fibrils with favorable parameters (aspect ratio ∼15) were obtained by simultaneous addition of all components or preblending of C15 in PCL, or by combination of both methods. On the other hand, application of the premade PLA/C15 and PLA/C30 nanocomposites leads to a negligible improvement of extrusion stability, which practically does not allow melt drawing. In this case, drawing was only possible with further addition of the clay together with all components. This indicates importance of clay affecting of the PCL phase. The effect of clay on rheology of the components and their 80/20 blend is shown below.

Table I indicates the effect of the clay on particle size in the undrawn sample [Figure 1(c,d)] and diameters of fibrils [Figure 1(a,b)] in the analogous melt-drawn systems. The addition of the clay decreases PLA particle size (900 nm); the most significant decrease in size to ∼300 nm was found for one-step added C30. Slightly less marked effect occurred for C15; similar size (∼400 nm) was found for both the one-step clay mixing and the PCL/C15 preblend application. Larger particles (∼600 nm) were found in the case of the PLA/C15 preblend application,

probably due to unfavorably increased viscosity and more difficult particle break-up, (confirming relatively higher clay content in PCL, at least in the early stage of mixing). Most probably, this effect leads to an unfavorable viscosity ratio and related hindered melt drawing mentioned above. It is obvious that, except of the well-known "interfacial activity" of clay,[21] the different affecting of components viscosity in the course of mixing and thus shearing forces seems to be also important.

The SEM analysis also shows comparable diameter of the PLA inclusions and fibrils, presented in Table I. From Figure 1(a), it is obvious that length of fibrils is ∼7 µm (aspect ratio ∼15). Such a drawing of inclusions of diameter ∼500 nm should lead to fibrils with significantly lower diameter (∼150 nm) than observed (Figure 1, Table I). As a result, the fibrils cannot be formed by mere drawing but some coalescence of these fibrils in the course of extrusion and melt drawing should also be considered, analogously to other MFCs with polyolefinic matrix.[30,43]

Clay Localization and Dispersion

Due to insufficient contrast and/or visualization of both phases in the samples for TEM, we were not able to evaluate clay localization in the systems studied. Taking into account the fact that localization of clay at the interface may provide "visualization" of components,[34] absence of this effect in the TEM images (Figure 2) may also indicate its limited interfacial localization. Figure 2 shows presence of lamellar stacks of C15 in combination with exfoliated platelets, in accord with the XRD analysis [Figure 3(a)]. Table II shows interfacial energies and wetting coefficients. Surface energy values and their dispersive and polar components[45] were extrapolated to values corresponding to 170°C using the temperature coefficient.

Taking into account low interfacial energies of both PLA and PCL with C15, relatively lower value for PLA, and wetting coefficient $x_{PLA} = 0.328$ (wetting coefficient[46] between 1 and −1), we can assume presence of the clay in both phases and at the interface, with possibly higher content in PLA. In the case of C30, the lower values of interfacial energy in comparison with C15 indicate improved affinity of both polymer components to the clay due to the more polar modifier of C30. The more marked decrease of interfacial energy for PLA and higher $x_{PLA} = 0.696$ (closer to 1) may indicate even more significant localization of this oMMT inside PLA. Moreover, the final oMMT localization may be influenced by its expected more significant localization in the PCL phase, at least in the early stages of mixing and drawing. The reason is the fact that the clay is first localized in earlier-melted PCL and then it migrates to later-melted PLA. This fact also corresponds to good fibril formation in the case of the PCL/clay preblend application. This indirectly confirms the presence of oMMT in PCL. Similarly, the predominant localization of clay inside PLA is practically excluded by the above mentioned impossible drawing in the case of the PCL/C15 and PCL/C30 preblends, i.e., in the system with expected preferred localization of clay inside the PLA phase. The XRD patterns in Figure 3(a) show relatively significant portion of intercalated C15 in MFC containing 2% clay indicated by the marked peak at 2θ position 2.38°
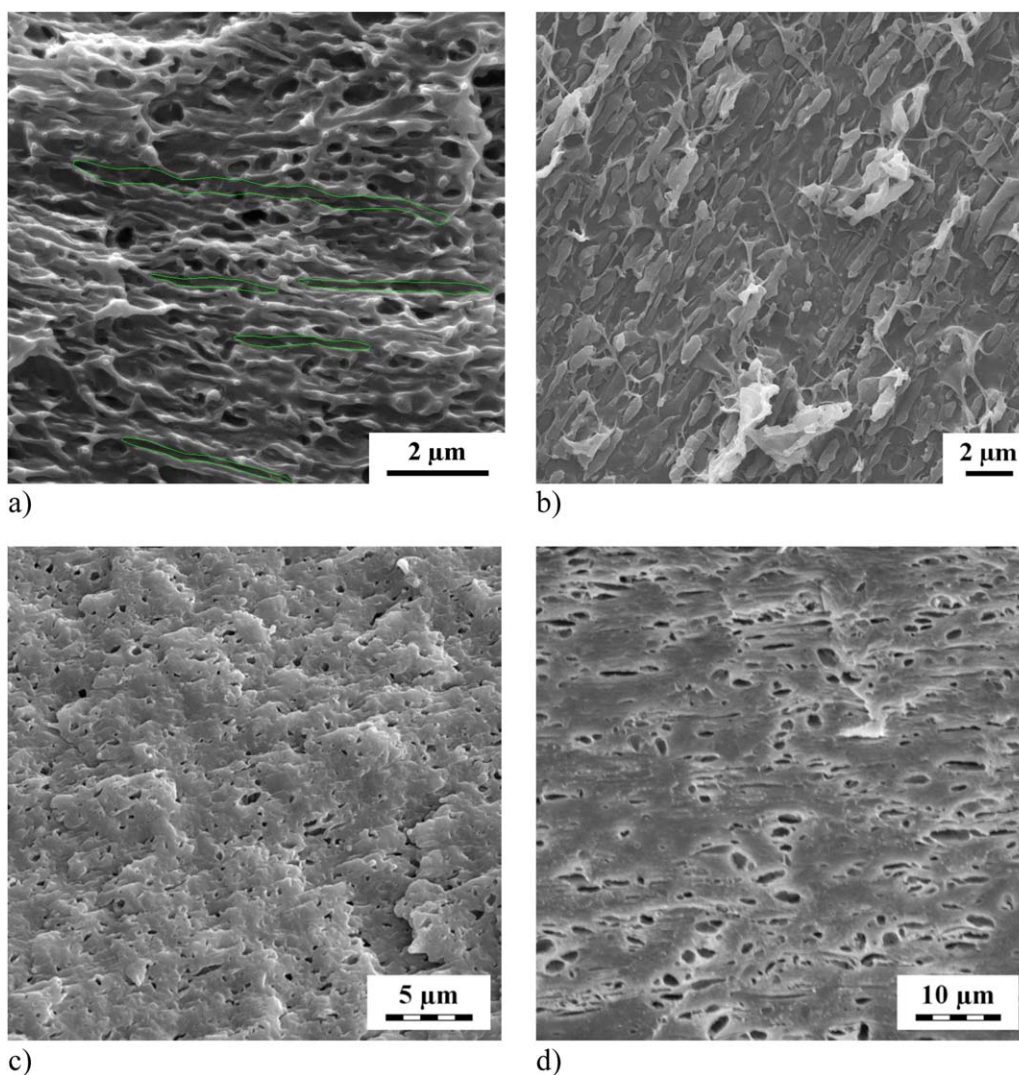
Figure 1. SEM images of (a) etched and (b) unetched melt drawn bristle of PCL/PLA/C15 80/20/2 system (draw ratio = 7); (c) undrawn injection-molded PCL/PLA/C15 80/20/2 system; (d) undrawn injection-molded PCL/PLA 80/20 blend. [Color figure can be viewed in the online issue, which is available at wileyonlinelibrary.com.]

corresponding to lamellar structure with interlayer distance $d001 = 3.71$ nm. Of importance is obvious higher degree of delamination due to drawing indicated by lower intensity of this peak. Figure 3(b) shows analogous MFC containing 2% C30; relatively low intensity of the peak at 2.64° with $d001 = 3.35$ nm indicates higher degree of exfoliation. This corresponds to higher affinity of the C30 clay with more polar modification to both PCL and PLA, as also indicated by lower interfacial energy in comparison with C15 (Table II). From Figure 3(b), it is obvious that the drawing increases the degree of C30 exfoliation, reflected in the decreased peak intensity.

Effect of Clay on Rheology of Components and MFC
The expected presence of clay in both phases (see above) undoubtedly changes their rheological parameters. The clay effect on flow behavior of single components at 170°C is apparent from Figures 4 and 5.

Table I. Effect of Clay on PLA Inclusion Size

Composition parts by wt.	Particle diameter (μm), undrawn sample	Fibril diameter (μm), draw ratio 7
PCL/PLA 80/20	0.9	–
PCL/PLA/C15 80/20/2	0.49	0.4
PCL/PLA/C30 80/20/2	0.24	0.24
PCL/(PLA/1%C30)[a] 80/20	0.66	–
(PCL/3%C15)[b]/PLA 80/20	0.45	0.4
(PCL/3%C15)[b]/ PLA/C15 80/20/3	–	0.36

[a] Premixed PLA nanocomposite.
[b] Premixed PCL nanocomposite.
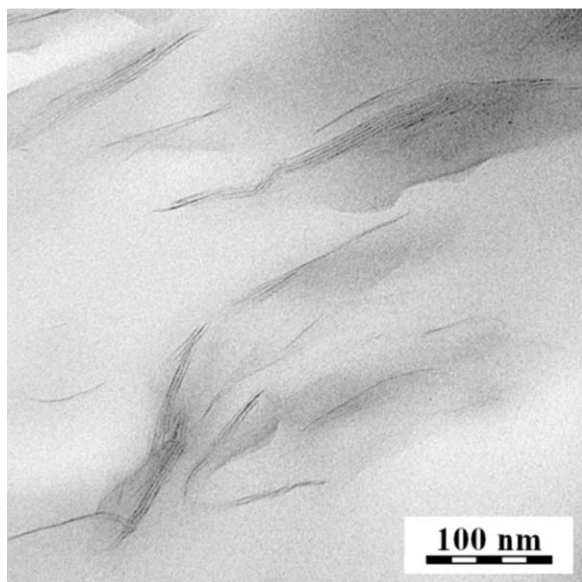
Figure 2. TEM image melt drawn PCL/PLA/C15 80/20/2 system (draw ratio = 7).

Table II. Interfacial Energies and Wetting Coefficients in PCL/PLA/oMMT System at Temperature 170°C

System	Interfacial energy (mJ m^{-2})	Wetting coefficient x_{PLA}
PLA/C15	3.198[a]	0.328[a]
	1.625[b]	0.327[b]
PLA/C30	0.548[a]	0.696[a]
	0.086[b]	0.697[b]
PCL/C15	3.763[a]	–
	1.91[b]	–
PCL/C30	1.748[a]	–
	0.693[b]	–
PCL/PLA	1.723[a]	–
	0.87[b]	–

[a] Harmonic mean equation.
[b] Geometric mean equation.[44]

Figure 4 shows that the addition of C15 increases viscosity (η^*) (and elasticity (G') —not shown for brevity) of PCL. It is obvious that 1% of C15 is dispersed in PCL in the form of individual particles. On the other hand, C15 starts forming physical network in the PCL/3%C15 nanocomposites, as documented by strong increase in η^* with decreasing ω in Figure 3. In contrast, addition of 1% of C15 to PLA leads to a slight decrease in η^* and G' in the whole range of ω (Figure 4), probably due to degradation.[47] Addition of 1% of C30 to PLA leads to slight increase in η^*, which matches up with the common idea of the effect of a small amount of individual particles. Figure 6 shows that the effect of C15 on rheological properties of the PCL/PLA 80/20 blends is similar to its effect on the properties of neat PCL. This demonstrates that substantial part of clay is localized in the PCL matrix, which controls rheological properties of the studied blends. From the above results, it follows that simultaneous affecting of both components or PCL alone by the clay leads to a more favorable ratio of components rheological parameters which support drawing. On the contrary, both increase in PLA viscosity due to C30 and decrease due to C15 in respective nanocomposites (Figure 4) is ineffective in

supporting fibril formation, as documented by practically impossible melt drawing in the case of both PCL/C15 and PCL/C30 preblends in combination with neat PCL. This confirms crucial importance of the PCL parameters. Moreover, the fact that drawing was also possible with low content <1% of the one-step added clay indicates that drawing can be achieved by relatively insignificant affecting of the PCL component parameters.

From Figure 7, it follows that the drawn samples (measured at 137°C to avoid melting of PLA fibrils), such as MFC PCL/PLA containing two parts of C15, show substantially larger values of complex viscosity, η^* and storage modulus, G', in the range of low ω than the analogous undrawn samples. From the well-known dependence of rheological properties of composites on the length to diameter ratio of dispersed fibers,[48] it clearly follows that the drawn samples contain more extended fibers than the related undrawn ones. This finding corresponds to the SEM observations (Figure 1).

Effect of Fibril Formation on Mechanical Properties
From Table III and Figure 8, it is apparent that mechanical properties of the drawn samples containing oMMT are substantially better in comparison with undrawn ones and the PCL matrix (Table IV). The best results were found in the case of
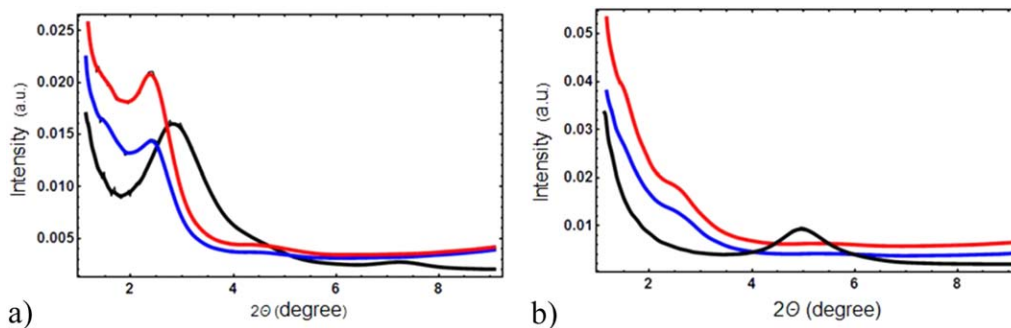

Figure 3. XRD patterns of systems containing (a) C15 and (b) C30. - neat oMMT, - PCL/PLA/oMMT 80/20/2 undrawn sample, - PCL/PLA/oMMT 80/20/2 MFC, draw ratio 7. [Color figure can be viewed in the online issue, which is available at wileyonlinelibrary.com.]
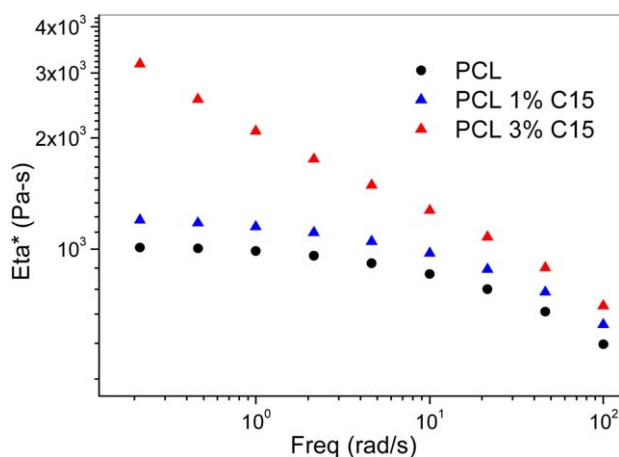
Figure 4. Effect of C15 addition on complex viscosity of PCL at 170°C. [Color figure can be viewed in the online issue, which is available at wileyonlinelibrary.com.]

the one-step addition of C15 and the application of the PCL/ C15 preblend. A relatively insignificant increase of parameters (E only) accompanied by reduced toughness of MFC with pre-made PCL/C15 with further C15 addition confirms the fact that optimum clay content is < 3%. Of predominant importance is the increase in yield stress and modulus which undoubtedly correspond to presence of well dispersed rigid PLA fibers [Figure 1(a)] and reinforcement of both phases by the clay. In the range of DR applied (5–7), the its effect on mechanical parameters was low. This is demonstrated for the sample containing 2% C15 in Table III. Further important contribution is higher crystallinity of dispersed/fibrillated PLA in MFC (∼25%) compared with PLA containing 1% C15 (∼ 9%), which leads to improved mechanical behavior.[49] Table IV shows ca 15% increase in E for bulk PLA and PLA/C15 with the mentioned increase in crystallinity achieved by annealing of the injection-molded dog-bone specimens at 70°C for 60 min. A more detailed study of the effect of fibrils and oMMT on crystallinity is in progress and will be published separately.[50] Figure 9 shows that experimental values of MFC moduli well correspond to or even exceed Hal-

Figure 6. Effect of C15 addition on complex viscosity of PCL/PLA 80/20 system at 170°C. [Color figure can be viewed in the online issue, which is available at wileyonlinelibrary.com.]

pin-Tsai[51] model calculations using E value of PCL/1%C15 NC, the modulus of PLA/1%C15 with higher (∼30%) crystallinity (Table IV), and aspect ratio ∼15. This matching of experimental
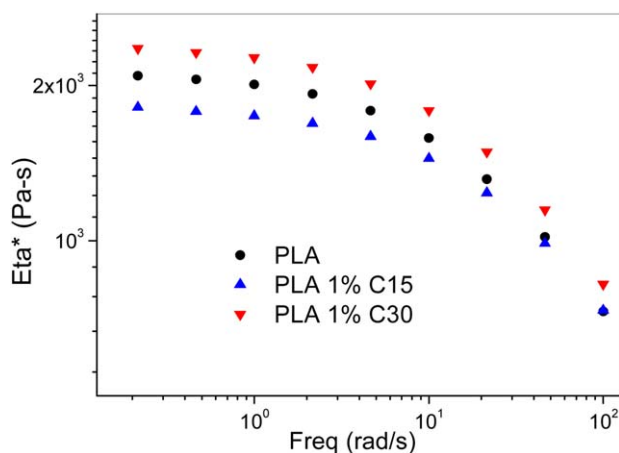

a)

Figure 5. Effect of oMMT addition on complex viscosity of PLA at 170°C. [Color figure can be viewed in the online issue, which is available at wileyonlinelibrary.com.]
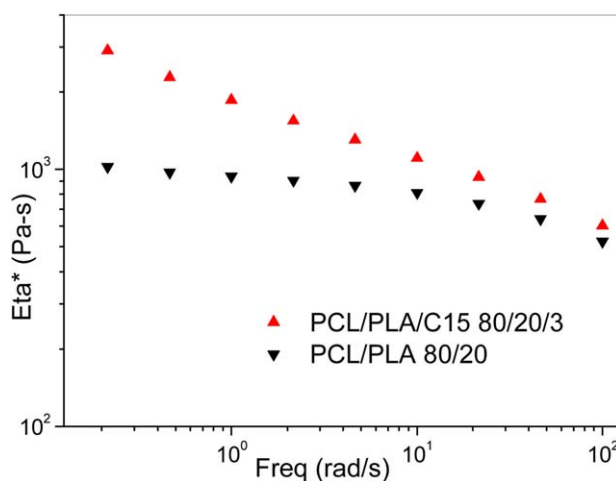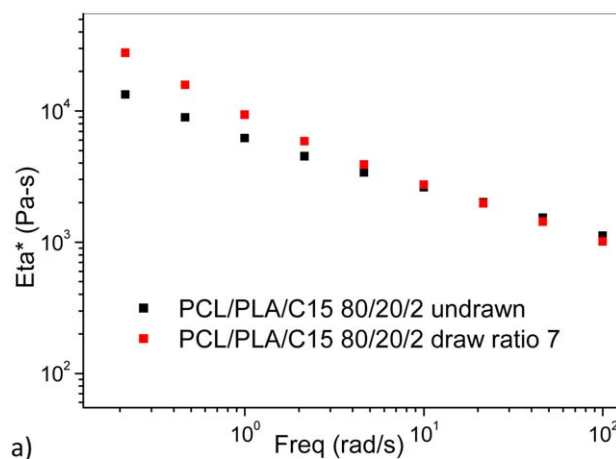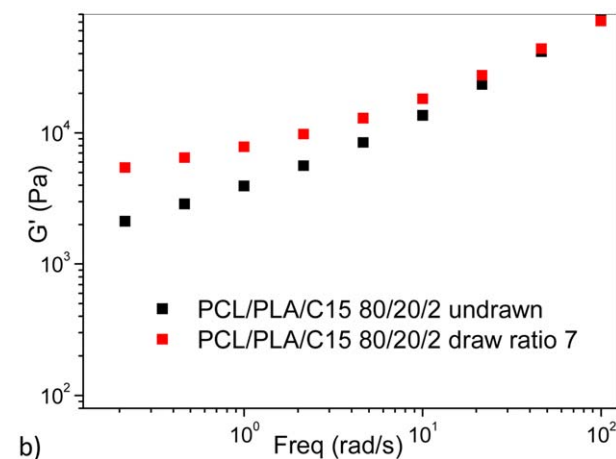
b)

Figure 7. Effect of C15 addition on (a) complex viscosity and (b) storage modulus of undrawn and melt drawn systems at 137°C. [Color figure can be viewed in the online issue, which is available at wileyonlinelibrary.com.]

Table III. Mechanical Properties of PCL/PLA 80/20 Blend in Dependence on Clay Content and Draw Ratio

Composition	DR	σ_y (MPa)	σ_b (MPa)	ε_y (%)	ε_b (%)	E (MPa)	a_t (kJ m^{-2})
PCL/PLA 80/20	1	20.2	26.8	7.6	295	720	60.8
PCL/PLA/C15 80/20/2	1	20.1	32.3	8	506	790	45
PCL/PLA/C15 80/20/2	5	22.4	35.6	8.6	428	930	46.3
PCL/PLA/C15 80/20/2	7	22.8	36.1	8.8	481	945	47
PCL/PLA/C30 80/20/2	1	22	30.5	7.6	422	560	45.6
PCL/PLA/C30 80/20/2	7	20.6	32.6	8	526	780	48.2
PCL/(PLA C15)[a] 80/20	1	22.5	25.5	7.9	244	650	62.4
PCL/(PLA C15)[a]/C30 80/20/2	1	22.4	31.6	7.5	405	780	54.4
PCL/(PLA C15)[a]/C30 80/20/2	7	22.3	33.4	7.7	434	870	59.5
(PCL C15)[b]/PLA 80/20	1	22.8	29.3	8.7	408	805	24.2
(PCL C15)[b]/PLA 80/20	7	23.4	32.7	9.3	438	945	31.6
(PCL C15)[b]/PLA/C15 80/20/2	1	21.3	31.7	7.8	540	830	20.7
(PCL C15)[b]/PLA/C15 80/20/2	7	23.05	29.9	9	394	995	22.8

Preblended components are in brackets.
[a] Preblend PLA/1% C15.
[b] Preblend PCL/3% C15.

and predicted values for AR 15 (estimated from Figure 1) indicates that AR may be close to this value. Moreover, agreement between experimental and predicted modulus occurs despite the fact that we used the Halpin-Tsai equation for an aligned composite whereas the injection-molded samples were not fully oriented; this indicates significant clay-reinforcement of components and possible higher "real" AR values. Moreover, AR effect on modulus in the range 15–30 is relatively less marked—see Figure 9. Some synergistic effects can also be considered. These may include influencing of parameters of the interface and increase of PLA parameters by melt drawing.

In MFC containing C30, the relatively lower strength and stiffness in comparison with analogous MFC containing C15 are in contrast with higher exfoliation of this clay (Figure 3), which

usually leads to increase in nanocomposites parameters.[47] This deterioration of properties corresponds most probably to lower AR of fibrils. According to Lai *et al.*,[52] deterioration of PLA parameters by the organomodifier at low content (∼1%) of (exfoliated) C30B clay can also be considered. Table III documents low effectivity of the premade PLA/15 NC application; its combination with neat PCL does not allow drawing. This was only possible with the simultaneously added clay; the relatively low parameters found are probably in correspondence to less effective drawing and the mentioned lower efficiency of C30 applied. The negative effect of preblending the clay with PLA, in spite of undoubted final clay localization inside the PLA phase in all MFCs studied, indicates important role of the clay migration from PCL to the PLA phase (see above) in the systems using the one-step addition of the clay or the PCL/C15 preblend in the course of mixing, extrusion, and melt drawing. The importance of the clay transfer is reflected in the best mechanical parameters of these systems (Table III). We expect favorable influencing of fibril formation and parameters of the interface due to the clay passing across the interfacial area in the course of MFC preparation, similarly to results found for
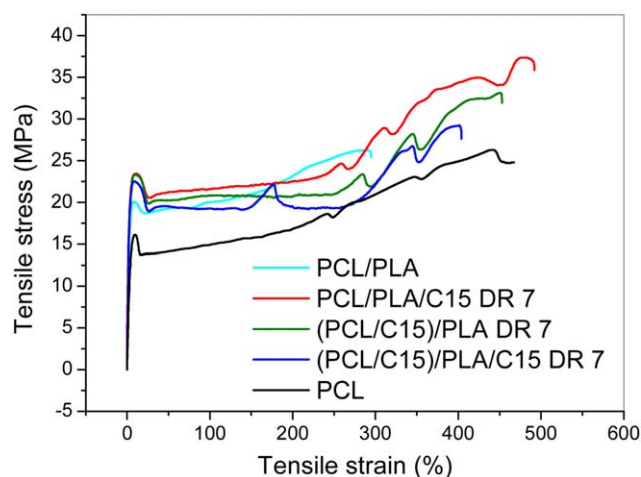

Figure 8. Stress–strain curves of PCL matrix, PCL/PLA 80/20 blend and related MFC containing 2% C15. (PCL/C15) means application of a preblend of PCL with 3% C15. [Color figure can be viewed in the online issue, which is available at wileyonlinelibrary.com.]

Table IV. Mechanical Properties of Polymer Components

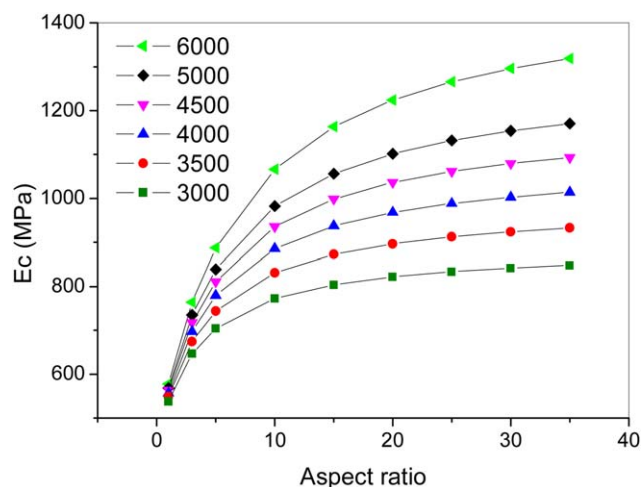| Composition	σ_y (MPa)	σ_b (MPa)	ε_y (%)	ε_b (%)	E (MPa)	a_t (kJ m^{-2})
PCL	16.1	27	9.4	472	310	80
PCL 1%C15	16.4	29.6	8.8	540	360	–
PCL 3%C15	16.7	32.8	7.7	672	435	–
PLA	68	–	2.65	4.3	3155	19
PLA[a]	69.7	–	3.1	4.05	3860	–
PLA1%C15[a]	70.8	–	2.35	4.1	4405	–
PLA 1%C15	69	–	2.6	5.22	3392	–

[a] Annealed 60 min at 70°C.

Figure 9. Effect of aspect ratio and modulus of fibers on stiffness of MFC; numbers inside the chart indicate PLA fiber modulus calculated using Halpin-Tsai model. E of PCL = 360 MPa. [Color figure can be viewed in the online issue, which is available at wileyonlinelibrary.com.]

HDPE/PA6 MFC.[34] The results indicate a more complex effect of clay on MFC behavior in comparison with the undrawn systems. Moreover, numerous clay-effects may be contradictory.[34] The E value of the undrawn system containing 2% C15 is relatively high ~790 MPa (Table III), which significantly exceeds the values of ~560 MPa predicted by Kerner's model[53] using the same matrix and fibrils moduli as in the Halpin-Tsai model calculations. Similar situation also occurs for the clay-free sample (experimental value of ~720 MPa, calculated ~490 MPa). Taking into account the strong effect of increasing AR in the range of 2–10 on modulus (Figure 9), the reason seems to be certain extent of PLA fibril formation with estimated AR ~4.5 (using Halpin-Tsai model) already in the undrawn sample due to flow through the extruder die. This is confirmed by the SEM observation of the undrawn sample [Figure 1(c,d)] showing important formation of the mentioned elongated inclusions with aspect ratio <5. Generally, all the above discussion, including the low correspondence of mechanical parameters like toughness to clay content, confirms the complex effect of clay exceeding the reinforcement of the components only. Unfortunately, more thorough discussion and understanding of these effects is limited by the impossibility to prepare analogous clay-free MFC.

CONCLUSIONS

The NF-modified PCL/PLA microfibrillar composites are a biodegradable material with broad potential range of applications. The results achieved clearly show that addition of oMMT enhances mechanical performance of MFC based on the melt-drawn 80/20 PCL/PLA blend. Of crucial importance is favorable affecting of components, especially rheological parameters of the PCL phase. This is the fact that makes melt drawing and thus *in situ* PLA fibrils formation possible. The improved mechanical behavior corresponds to the micron-sized fibrils formation and oMMT reinforcement of both polymer components as well as to increased crystallinity of the fibrillar PLA phase.

The experimental values of modulus correspond to or even exceed the values predicted by the Halpin-Tsai model. This indicates possible synergistic effect of oMMT-modified polymer components and the interface parameters on the MFC performance. From the results obtained, it follows that the role of oMMT in MFC is quite complex; this corresponds to the best results obtained in the case of the less exfoliated clay with lower affinity to the polymer components. Numerous clay-induced effects may be contradictory and must be harmonized to achieve PCL-based biodegradable MFCs with improved parameters.

REFERENCES

1. Woodruff, M. A.; Hutmacher, D. W. *Prog. Polym. Sci.* **2010**, *35*, 1217.

2. Simões, C. L.; Viana, J. C.; Cunha, A. M. *J. Appl. Polym. Sci.* **2009**, *112*, 345.

3. Yeh, J. T.; Wu, C. J.; Tsou, C. H.; Chai, W. L.; Chow, J. D.; Huang, C. J.; Chen, K. N.; Wu, C. S. *Polym. Plast. Technol. Eng.* **2009**, *48*, 571.

4. Newman, D.; Laredo, E.; Bello, A.; Grillo, A.; Feijoo, J. L.; Müller, A. *J. Macromolecules* **2009**, *42*, 5219.

5. López-Rodríguez, N.; López-Arraiz, A.; Meaurio, E.; Sarasua, J. R. *Polym. Eng. Sci.* **2006**, *46*, 1299.

6. Na, Y. H.; He, Y.; Shuai, X.; Kikkawa, Y.; Doi, Y.; Inoue, Y. *Biomacromolecules* **2002**, *3*, 1179.

7. Tuba, F.; Olah, L.; Nagy, P. *Eng. Fract. Mech.* **2011**, *78*, 3123.

8. Ju, D.; Han, L.; Li, F.; Chen, S.; Dong, L. *Polym. Compos.* **2013**, *34*, 1745.

9. Neppalli, R.; Marega, C.; Marigo, A.; Bajgai, M. P.; Kim, H. Y.; Causin, V. *Polymer* **2011**, *52*, 4054.

10. Neppalli, R.; Marega, C.; Marigo, A.; Bajgai, M. P.; Kim, H. Y.; Causin, V. *Eur. Polym. J.* **2010**, *46*, 968.

11. Chen, B.; Sun, K.; Ren, T. *Eur. Polym. J.* **2005**, *41*, 453.

12. Teramoto, N.; Urata, K.; Ozawa, K.; Shibata, M. *Polym. Degrad. Stabil.* **2004**, *86*, 401.

13. Qiao, X.; Li, W.; Watanabe, H.; Sun, K.; Chen, X. *J. Polym. Sci. B: Polym. Phys.* **2009**, *47*, 1957.

14. Chen, J.; Lu, L.; Wu, D.; Yuan, L.; Zhang, M.; Hua, J.; Xu, J. *ACS Sustainable Chem. Eng.* **2014**, *2*, 2102.

15. Chen, B.; Evans, J. R. G. *Macromolecules* **2006**, *39*, 747.

16. Labidi, S.; Azema, N.; Perrin, D.; Lopez-Cuesta., J. M. *Polym. Degrad. Stabil.* **2010**, *85*, 382.

17. Moyo, L.; Makhado, E.; Sinha Ray, S. *J. Appl. Polym. Sci.* **2014**, *131*, 41109.

18. Chrissafis, K.; Antoniadis, G.; Paraskevopoulos, K. M.; Vassiliou, A.; Bikiaris, D. N. *Compos. Sci. Technol.* **2007**, *67*, 2165.

19. Lee, K. S.; Chang, Y. W. *J. Appl. Polym. Sci.* **2013**, *128*, 2807.

20. Neppalli, R.; Causin, V.; Marega, C.; Saini, R.; Mba, M.; Marigo, A. *Polym. Eng. Sci.* **2011**, *51*, 1489.

21. Gelfer, M. Y.; Song, H. H.; Liu, L.; Hsiao, B. S.; Chu, B.; Rafailovich, M.; Si, M.; Zaitsev, V. *J. Polym. Sci. B: Polym. Phys.* **2003**, *41*, 44.

22. Kelnar, I.; Sukhanov, V.; Rotrekl, J.; Kaprálková, L. *J. Appl. Polym. Sci.* **2010**, *116*, 3621.

23. Kelnar, I.; Khunová, V.; Kotek, J.; Kaprálková, L. *Polymer* **2007**, *48*, 5332.

24. Jain, S.; Reddy, M. M.; Mohanty, A. K.; Misra, M.; Ghosh, A. K. *Macromol. Mater. Eng.* **2010**, *295*, 750.

25. Wu, D.; Lin, D.; Zhang, J.; Zhou, W.; Zhang, M.; Zhang, Y.; Wang, D.; Lin, B. *Macromol. Chem. Phys.* **2011**, *212*, 613.

26. Hasook, A.; Tanoue, S.; Iemoto, Y.; Unryu, T. *Polym. Eng. Sci.* **2006**, *46*, 1001.

27. Li, Q.; Yoon, J. S.; Chen, G. X. *J. Polym. Environ.* **2011**, *19*, 59.

28. Jayanarayaran, K.; Thomas, S.; Joseph, K. *J. Polym. Res.* **2011**, *18*, 1.

29. Yi, X.; Xu, L.; Wang, Y. L.; Zhong, G. J.; Ji, X.; Li, Z. M. *Eur. Polym. J.* **2010**, *46*, 719.

30. Fakirov, S.; Bhattacharyya, D.; Lin, R. J. T.; Fuchs, C.; Friedrich, K. *J. Macromol. Sci. Phys.* **2007**, *46*, 183.

31. Li, Z. M.; Li, L. B.; Shen, K. Z.; Yang, W.; Huang, R.; Yang, M. B. *Macromol. Rapid. Commun.* **2004**, *25*, 553.

32. Yesil, S.; Bayram, G. *J. Appl. Polym. Sci.* **2013**, *127*, 982.

33. Lin, R. J. T.; Bhattacharyya, D.; Fakirov, S. *Int. J. Mod. Phys.* **2010**, *B 24*, 2459.

34. Kelnar, I.; Kaprálková, L.; Kratochvíl, J.; Kotek, J.; Kobera, L.; Rotrekl, J.; Hromádková, J. *J. Appl. Polym. Sci.* **2015**, *132*, 41868.

35. Thomason, J. L. *Polym. Compos.* **2007**, *28*, 331.

36. Ishida, H.; Chaisuwan, T. *Polym. Compos.* **2003**, *24*, 597.

37. Liu, P.; Zhu, K.; Ouyang, Y.; Xiao, R. *J. Appl. Polym. Sci.* **2013**, *130*, 2832.

38. Friedrich, K.; Hoffmann, J.; Evstatiev, M.; Ye, L.; Mai, Y. W. *Key Eng. Mater.* **2007**, *334–335*, 1181.

39. Kimble, L. D.; Bhattacharyya, D.; Fakirov, S. *Express Polym. Lett.* **2015**, *9*, 300.

40. Simeonova, S.; Evstatiev, M.; Li, W.; Burkhart, T. *J. Polym. Sci. B Polym. Phys.* **2013**, *51*, 1298.

41. Lu, L.; Wu, D.; Zhang, M.; Zhou, W. *Ind. Eng. Chem. Res.* **2012**, *51*, 3682.

42. Haroosh, H. J.; Dong, Y.; Chaudhary, D. S.; Ingram, G. D.; Yusa, S. I. *Appl. Phys. A: Mater. Sci. Process.* **2013**, *110*, 433.

43. Kelnar, I.; Fortelný, I.; Kaprálková, L.; Hromádková, J. *Polym. Eng. Sci.* **2015**, *55*, 2133.

44. Wu, S. Polymer Interface and Adhesion; Marcel Dekker Inc.: New York, **1982**.

45. Taguet, A.; Cassagnau, P.; Lopez-Cuesta, J. M. *Prog. Polym. Sci.* **2014**, *39*, 1526.

46. Sumita, M.; Sakata, K.; Asai, S.; Miyasaka, K.; Nakagawa, H. *Polym. Bull.* **1991**, *25*, 265.

47. Giannelis, E. P.; Krishnamoorti, R.; Manias, E. *Adv. Polym. Sci.* **1999**, *138*, 107.

48. Vinogradov, G. V.; Malkin, A. Y. Rheology of Polymers; Mir Publishers: Moscow, **1980**; p 380.

49. Liu, G.; Zhang, X.; Wang, D. *Adv. Mater.* **2014**, *26*, 6905.

50. Kelnar, I.; Kratochvíl, J.; Kaprálková, L. *J. Therm. Anal. Calorim.* **2015**, submitted.

51. Halpin, J. C.; Kardos, J. L. *Polym. Eng. Sci.* **1976**, *16*, 344.

52. Lai, S. M.; Wu, S. H.; Lin, G. G.; Don, T. M. *Eur. Polym. J.* **2014**, *52*, 193.

53. Kerner, E. H. *Proc. Phys. Soc.* **1956**, *69*, 808.